Article:
Laity, P.R., Baldwin, E. and Holland, C. (2019) Changes in silk feedstock rheology during cocoon construction: the role of calcium and potassium ions. Macromolecular Bioscience, 19 (3). ISSN: 1616-5187

https://doi.org/10.1002/mabi.201800188

Macromolecular Bioscience
www.mbs-journal.de

Changes in Silk Feedstock Rheology during Cocoon Construction: The Role of Calcium and Potassium Ions

Peter R. Laity, Elizabeth Baldwin, and Chris Holland**

Variation in silk feedstocks is a barrier both to our understanding of natural spinning and biomimetic endeavors. To address this, compositional changes are investigated in feedstock specimens from the domesticated silkworm (*Bombyx mori*). It is found that the feedstock viscosity decreased systematically by over two orders of magnitude during cocoon construction. Potential factors such as protein concentration, molecular weight, pH, or the presence of trehalose are excluded, whereas a clear correlation appear between viscosity and the relative concentrations of Ca^{2+} and K^{+} ions. It is expected that Ca^{2+} ions would favor "salt bridges" between acidic (Asp and Glu) amino acids, leading to an increased viscosity, whereas K^{+} ions would compete for these sites, thereby reducing viscosity. Thus, these findings suggest a simple, systematic yet sophisticated control of feedstock viscosity in the silkworm, which in turn can be applied to future industrial silk production.

1. Introduction

Variation in silk is often perceived to be a barrier both to our understanding of natural spinning and successful biomimetic implementation of similar methods. While factors affecting fiber properties are now largely understood, variation in the unspun protein feedstock is not. This is addressed in the present study.

Silk fibers are produced by a diverse range of arthropods including, most notably, true spiders and caterpillars (lepidopteran larvae).[1–8] Many of these fibers exhibit remarkable modulus, strength, and toughness, rivalling high performance man-made fibers.[6–11] Moreover, they are produced under physiological conditions, from an aqueous protein solution (feedstock) that is prepared and stored inside the animal at ambient temperatures, without large energy inputs, or use of harmful chemicals.[12] It is generally believed that this remarkable conversion from the liquid feedstock to the solid fiber is initiated largely by (shear and extensional) flow through the silk duct.[13–16] Indeed, previous work[17] demonstrated that flow stress alone was sufficient to initiate gelation on a rheometer—although that did not preclude possible additional roles of compositional changes (e.g., pH or salts) in the natural process.

Rather surprisingly for a process initiated by flow, however, dramatic variations in the rheology of silk feedstocks have been observed. Using specimens prepared in a consistent way from closely related silkworms at a (nominally) similar life-cycle stage (using middle-posterior gland contents from 5th instar *Bombyx mori* larvae at the start of cocoon construction), the shear viscosity (η_1) measured at a shear rate ($\dot{\gamma}$) of 1 s^{-1} ranged from around 50 to over 6000 Pa s.[18,19] While a small part of this rheological variation may be related to observed changes in the solids content of the feedstock (from ≈18 to 30 wt%), a definitive explanation for the largest part remains elusive.

Changes in viscosity, silkworm body mass, and analyses of feedstock composition using a range of techniques are reported here. This revealed a systematic decrease in viscosity over two orders of magnitude during the course of cocoon construction, which correlated to the relative concentrations of calcium and potassium ions. A more detailed discussion of the rheological effects will be presented in the subsequent paper by Schaefer et al.[20] From a biological perspective, these changes may be associated with switching the feedstock from fibroin production and storage to fiber spinning. Moreover, understanding the interactions between dissolved ions and fibroin may have relevance for industrial processing of reconstituted (i.e., redissolved, native) or biomimetic silk proteins.

2. Experimental Section

Experiments were performed using commercially bred *B. mori* silkworms (four-way poly-hybrid cross of two Japanese and two Chinese strains). The animals were received at around 5 days into their 5th instar and individually housed in ventilated 50 mL plastic centrifuge tubes at room temperature (≈22 ± 2 °C) until required. The body masses of individual specimens at the start of the experiment appeared to be normally distributed, with mean 3.25 g and standard deviation 0.45 g, as shown in **Figure 1**a.

Specimens were also weighed prior to sacrifice, in order to observe the changes in body mass. Although at (nominally) the same developmental stage, significant variations were observed

Dr. P. R. Laity, Dr. E. Baldwin, Dr. C. Holland
Department of Materials Science and Engineering
University of Sheffield
Sir Robert Hadfield Building, Mappin Street, Sheffield S1 3JD, UK
E-mail: petelaity@aol.com; christopher.holland@sheffield.ac.uk

The ORCID identification number(s) for the author(s) of this article can be found under https://doi.org/10.1002/mabi.201800188.

DOI: 10.1002/mabi.201800188

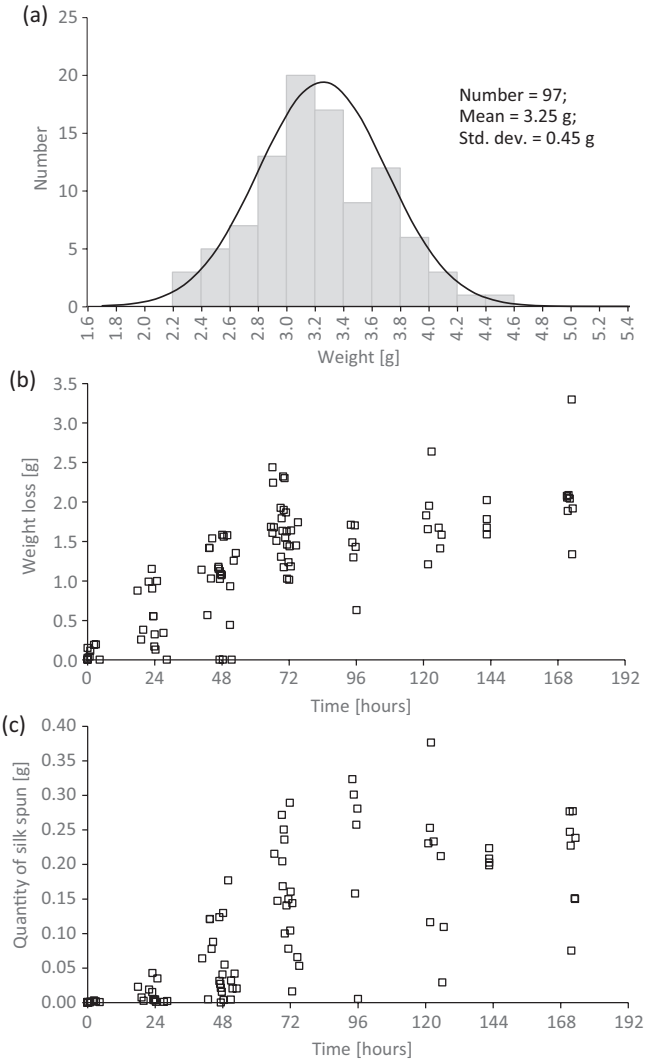

Figure 1. a) Weights of silkworms at the start of the experiment: the histogram shows the measured population, while the continuous line shows the normal distribution with mean 3.25 g and standard deviation 0.45 g; b) weight loss observed and c) quantities of silk fiber produced against time, during the experiments.

in both the changes in body mass and the rates at which silk fiber was produced (Figure 1b,c). Consequently, the quantity of silk produced was used as a direct metric for progress through cocoon construction. This was estimated after manually removing from the tube, separating from the silkworm and any feces, then drying under vacuum at around 60 °C.

Silkworms were sacrificed by rapidly removing the head using scissors, which allowed the pair of silk glands to be ejected onto a petri dish, together with the hemolymph. The pH of the hemolymph was measured using narrow range indicator paper strips (±0.5 pH units) and a micro-electrode (CupFET 3200-010 pH probe with SI600 meter, Sentron, The Netherlands).

One silk gland was transferred to a second dish and gently washed by covering with "type 1" (distilled and deionized) water. Using fine tweezers, a cut was made about half way along the middle division in the middle (MM) section and the "downstream" part, which contained a larger sericin content, was discarded. The thin posterior (P) section was also cut off and discarded (**Figure 2**a,b). The silk feedstock was exposed by carefully peeling off the epithelial membrane, using tweezers and a dissection microscope. The pH was checked using the micro-electrode and then further portions of the feedstock were removed for analysis, as described below in sections 2.1 to 2.5.

Where possible, all subsequent measurements (rheology, solids content, and spectroscopic analyses) were performed using samples from the MP section of the same gland. Where this was not possible, due to the diminishing sizes of silk glands during cocoon construction, some measurements were omitted or performed on the MP section of the second gland. The experiments were continued over periods of several days (typically 3 to 7, depending on rate at which the worms gave silk), which encompassed the wandering stage and most of cocoon building (e.g., as shown in Figure 2c–f), until the glands were too empty to permit further measurements.

2.1. Rheology

A small portion of silk feedstock (≈0.01–0.02 g) from about halfway along the MP section (see Figure 2a,b) was gently placed onto the rheometer (Bohlin Gemini, Malvern Instruments, UK) fitted with a CP 1/10 geometry (10 mm diameter cone with 1° opening angle and 30 μm truncation). A constant shear rate of 1 s^{-1} was applied over 100 s at 25 °C and the shear viscosity was determined by averaging data from the final 30 s, as described previously.[19]

2.2. Infrared Spectroscopy

Infrared (IR) spectra were collected from protein films using both transmission and attenuated total reflectance (Golden Gate 45° "single bounce" diamond ATR device, Specac, UK) modes. In order to maximize the sensitivity for the bands of interest and avoid various potential errors that can arise in ATR measurements,[21–24] however, the present analyses were based on transmission spectra from thin films (≈10 μm thickness).

Samples were prepared by weighing a second feedstock specimen from the MP section (up to 0.2 g) into a small tared plastic (polystyrene) weighing boat, together with a small portion of type 1 water (≈2 mL); this was loosely covered with paper tissue and allowed to stand at room temperature. Over a few days, the silk feedstock dissolved and then the resulting solution gradually dried out to produce a thin film. Final drying was achieved under vacuum at 60 °C. Note: comparisons with films prepared using only drying in ambient air suggested that, other than removing the last traces of absorbed water, such treatment did not significantly affect the spectra obtained.

Films were mounted in the transmission sample holder of the spectrometer (Nicolet 360, Thermo Electron Corp, Madison, WI, USA) using a cardboard support. In order to ensure consistency, IR spectra were collected (by Fourier Transform,

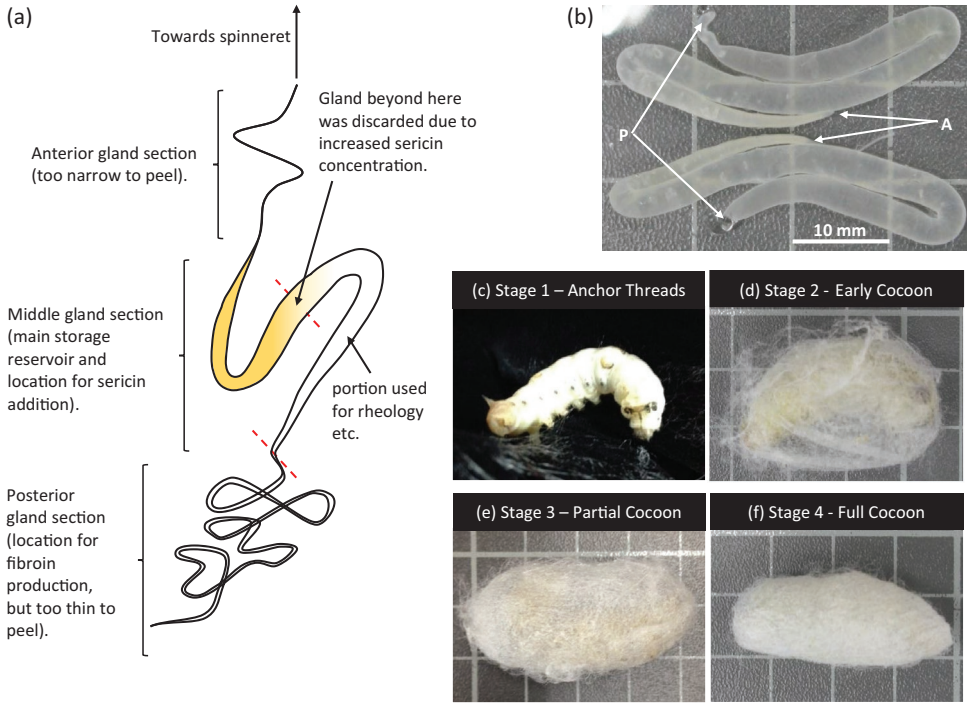

Figure 2. Description of typical specimens; a) diagram showing parts of a silk gland and origins of the samples used (dashed lines demark where the gland was cut); b) photograph of middle gland sections (A and P indicate where it joined the anterior and posterior sections); c–f) arbitrary stages of cocoon construction (anchor lines only to full cocoon).

using 64 scans at 1 cm^{-1} resolution) in triplicate, with the film repositioned slightly between acquisitions. These specimens generally absorbed too strongly to observe the most intense bands (i.e., the N—H stretching and amide bands of the peptides), but produced very clear spectra of the weaker bands, including the "fingerprint" region. To compensate for differences in film thickness, the spectra in the fingerprint region (800–1500 cm^{-1}) were normalized against the amide III band (1243 cm^{-1}), which was expected to be a constant feature in each of the silk protein specimens.

2.3. Protein Analysis by Gel Electrophoresis

Small portions of silk feedstock (0.01–0.02 g, from the MP section, near the rheology sample) were weighed into 2 mL plastic sample vials and allowed to dissolve in distilled water overnight in a refrigerator. The resulting solutions were further diluted to 1 mg mL^{-1}, then mixed with an equal volume of a solution containing sodium dodecyl sulfate (SDS, 4 %, to disrupt non-covalent bonding) and 2-mercaptoethanol (4 mM, to reductively cleave disulfide bonds in the proteins). Aliquots of the resulting analyte solutions (10 µL, equivalent to 10 µg of protein) were loaded onto on a 4–20 % polyacrylamide (PA) gradient gel and the protein components were separated by electrophoresis (GE), over 90 min. at 160 V and 100 mA. After fixing the gel (by immersion in a solution of ethanol 400 mL, ethanoic acid 100 mL, and water 500 mL over 30 min.), protein bands were stained by Coomassie blue and imaged using a Perfection 2450 Photo scanner (Seiko Epson Corp. Suwa, Japan) at 1200 DPI. Molecular weights of the analytes were calculated by comparing their movement with reference standards (pre-colored Full-range and Hi-mark protein).

2.4. Gravimetric Estimation of Protein Concentration

Where a sufficient amount of the film prepared for IR was available, the solids content (predominantly protein) of the silk feedstock could be determined from this. Otherwise, the remainder of each (MM and MP) silk gland not required for rheology, IR or GE was weighed onto a tared piece of aluminium foil and the solid residue was determined gravimetrically, after drying to constant weight in a vacuum oven (at 60 °C).

2.5. Elemental Analysis

Finally, after collecting IR spectra and measuring the dry weight, film specimens (minimum ≈0.03 g) were dissolved using a solution (3.0 mL) of ethylenediamine-tetraacetic acid and tetramethylammonium hydroxide (EDTA + TMAH). The concentrations of the major elements (other than C, H, N, and O) were determined by inductively coupled plasma optical emission spectroscopy (OES, Spectro-Ciros Vision, Ametek Inc. Mahwah, NJ, USA). Note that pilot experiments demonstrated that similar results were obtained using dissolution in EDTA + TMAH or a more aggressive mixture of nitric and perchloric acids.

3. Results

3.1. Determining Cocoon Construction Progress

Examples of four qualitative stages of cocoon construction (anchor lines only, early, partial, and complete) are shown in Figure 2c–f. Although the silkworms were received at (nominally) the same age (around 5 days into the 5th instar), this was regarded as too arbitrary a starting point, since it made no allowance for possible differences in development rates. Although the subsequent changes in body mass (Figure 1b) or quantity of silk produced (Figure 1c) followed the expected trends, they showed poor correlations. Hence, it appeared that the time from the start of 5th instar, as used elsewhere,[25] may not provide a sufficiently reliable, quantitative metric for cocoon construction. Instead, it was considered that a direct measurement of the silk fiber produced by the silkworm would be more appropriate.

3.2. Changes in Viscosity during Cocoon Construction

Over the entire study, viscosity measurements from different individuals were found to be extremely widely distributed, as shown in **Figure 3**a. Although the greatest abundance was found between 500 and 1000 Pa s, individual samples were observed with viscosities below 100 Pa s or above 7000 Pa s. It may be noted that this range was even more extreme than that reported previously.[18,19] Moreover, if these results were truly representative of the feedstock being used by the silkworm, they raise the obvious questions of how fibers could be spun from feedstock with such variable flow behavior, particularly in view of the physiological constraints discussed recently by Sparkes and Holland.[13] Yet, in all cases, the measurements appeared reliable, with no evidence of gland membrane debris or premature gelation, due to poor dissection technique.

Closer examination revealed, however, that this was not the result of random variability. Plotting the viscosity against the quantity of silk fiber produced (Figure 3b) revealed a systematic decline as cocoon construction progressed. This may indicate changes in the feedstock from storage conditions to a spinnable material, and begs an explanation for how the silkworm achieves this. Investigations into a number of potential mechanisms are presented below.

3.3. Changes in pH and Solids Content during Cocoon Construction

Changes were observed (by indicator paper and micro-electrode) in the hemolymph pH, which was elevated at the start of the experiments (>9, as indicated by the filled points in Figure 3b), but subsequently decreased (5–7) prior to the onset of fiber production. This was consistent with previous work by Hirayama et al.[26,27] which revealed an interesting method that *B mori* silkworms use to recycle nitrogen from urea (normally a waste product) into ammonia as a resource for protein synthesis.

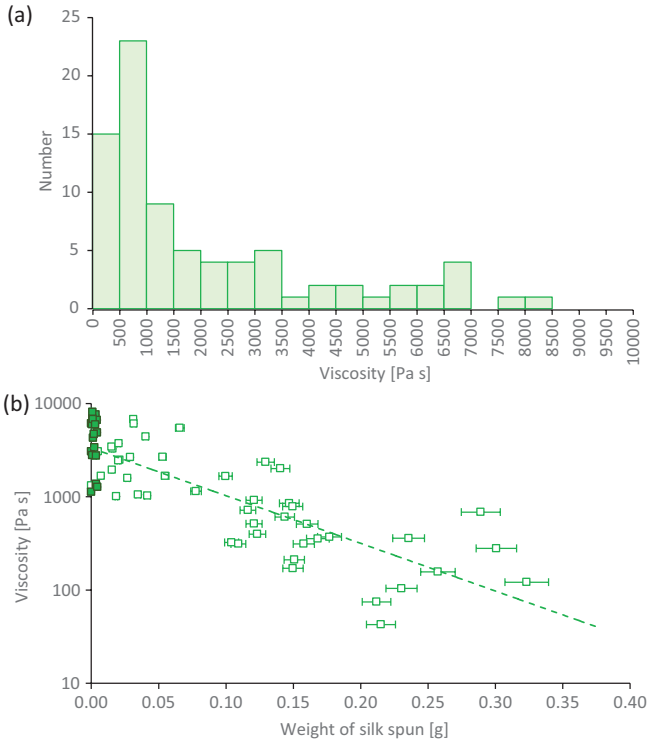

Figure 3. a) Overall distribution of viscosities measured during the experiments; b) viscosity plotted against the quantity of silk produced, indicating a downward trend as cocoon construction progressed. The filled points in (b) indicate where the hemolymph pH was elevated (>9), while the open points indicate where it was mildly acidic (5–7). It should be noted, though, that no corresponding changes were observable within the silk feedstock itself, which remained close to neutral (6.5–7.2). The dashed line represents the best fit (using an exponential trendline), but no physical meaning is suggested at present and it may be regarded as merely a guide for the eye. The horizontal error bars (±5 %) in (b) represent the uncertainty in determining the quantity of silk produced, after collecting from the inside of the specimen tube and disentangling any pellet of feces.

Based on the published amino acid sequence,[28–32] fibroin is believed to contain small proportions of phenolic, carboxylic acid, or amine substituents in the side-groups (≈5.2, 1.4, and 0.9 mol%, respectively). Previous work has suggested that interactions between these groups are sensitive to pH, thereby affecting the fibroin chain conformation and viscosity.[33–40] Indeed, rheological changes brought about by exposing silk feedstock to ethanoic acid or ammonia vapors have previously been reported by Terry et al.[41]

Nevertheless, the present work revealed no direct correlation between the hemolymph pH and the measured viscosity, as shown in Figure 3b. Moreover, the pH of the feedstock appeared to remain roughly neutral (6.5 to 7.2), in agreement with previous work[33] and suggesting that the gland contents are insulated from changes in the hemolymph.

The solids (predominantly fibroin) content of the silk feedstock was around 25 wt% at the start of the experiments, but declined slowly to around 16 wt% during cocoon construction, as shown in **Figure 4**a. It is unclear whether this serves a purpose for the silkworm or is merely the unavoidable consequence of using up its fibroin. This modest decrease in solids content may

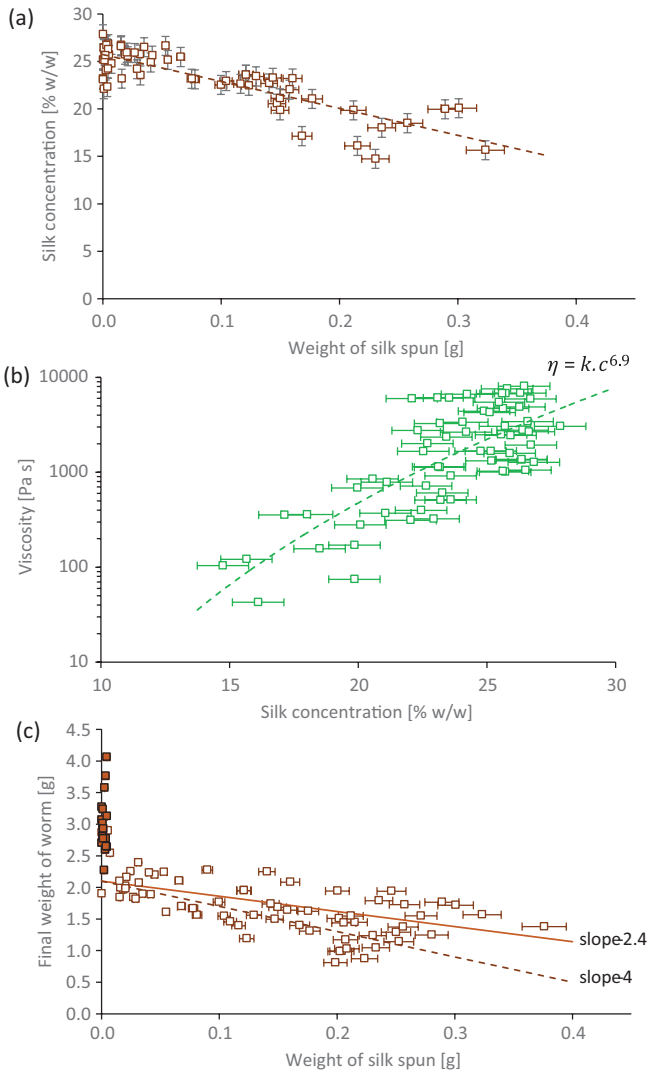

Figure 4. a) Solids content of silk feedstock during cocoon construction (the vertical error bars (±1%) represent the uncertainty based on the "worst case" weighing errors expected with the smallest specimens used; the line merely provides a guide for the eye); b) viscosity versus solids content (the dashed line represents the best fit using a power law); c) silkworm body mass at sacrifice (hemolymph pH was 9–10 for the filled points and 5–7 for the others (the continuous line with a slope of −2.4 represents a linear regression line through the data after the "gut purge," while the dashed line has a slope of −4, which would be consistent with the expected change due to the silkworm extruding a 25 % w/w feedstock into fiber).

account for some reduction in viscosity, as noted previously;[19] however, it appears unlikely to fully explain the roughly two orders of magnitude decrease in viscosity observed, especially if the silk feedstock obeys classical polymer solution behavior. Plotting viscosity against concentration (Figure 4b) revealed a relatively weak correlation ($R^2 = 0{\cdot}59$) to a power law relation:

$$\eta = kc^{6.9} \quad (1)$$

where c represents concentration and k is a constant ($= 4.91 \times 10^{-7}$, for c in wt%). First, the spread of data in this plot was significantly greater than the expected experimental uncertainty, suggesting that additional factors were involved. Second, for polymers in good solvents, the reptation model[42] and other theoretical treatments[43] predict a power law exponent around 3.75, which is largely supported by numerous experimental observations of polymer solutions.[44–46]

These measurements of gland concentration and weight of silk spun led to additional observations. First, the raised hemolymph pH (filled points in Figure 3c) preceded the start of silk production and coincided with a steep drop in body mass, which can be linked to the "gut purge" (ejection of feces and urine) that the silkworms undergo prior to cocoon construction. Subsequently, based on the initial protein content (25 wt%) in the feedstock, it would be expected that a plot of body mass against fiber mass should follow a slope of at least −4 (i.e., 0.4 g of feedstock extruded produces 0.1 g of dry fiber). Fitting a linear regression to the data after the gut purge in Figure 3 suggested a lower slope (≈−2·4), however, which may indicate that the silkworms recover some (roughly half) of the water from the feedstock, within the anterior parts of their silk glands. This may be consistent with water being expelled from the nascent fiber inside the animal, providing a potential mechanism for its retention, while forming a low viscosity lubricating layer within the duct to assist with silk pultrusion.[13]

3.4. Trace Element Analysis

In addition to the main elements (C, H, N, and O) found in proteins, significant amounts of other elements have been observed previously in silk feedstocks and fibers.[47–49] In particular, K and Ca were the most abundant (up to several milligrams per gram), with smaller amounts of Mg, Mn, Fe, Si, P, S, Cl, and Cu reported. Moreover, it has been suggested that several of these ions could affect the protein conformation or intermolecular interactions in solution;[14,15,36,37,47–49] hence, rheological effects may be expected.

Applying OES to analyze feedstocks from silkworms at different degrees of cocoon construction revealed stark differences in elemental composition. Although the method was capable of observing a wider range of elements, only Ca, K, Mg, Na, P, and S were consistently found in appreciable amounts (from around 10 to 3500 ppm by weight on dry residue, corresponding to roughly 0.1 to 55 atoms per fibroin chain of the expected 420 kDa molecular weight). The results for these elements are summarized in **Figure 5**.

Relatively large amounts of divalent cations (around 28 Ca^{2+} and 2 Mg^{2+} ions per chain) were found consistently in the feedstock specimens, irrespective of their viscosity (Figure 5a). Studies of ion exchange equilibria[54,55] have demonstrated that divalent cations have strong affinities for carboxylate anions. Hence, it is likely that these cations could bridge between fibroin molecules, which are expected to contain around 77 acidic amino acids (Asp and Glu) per chain,[32] in addition to any other potential ligand groups (e.g., phosphate or sulfate esters[50–53]) that may be present. Indeed, it may be noted that the mechanical properties of caddisfly silks, which are normally produced and used under water, appear to depend strongly on the presence of Ca^{2+} ions.[56] Importantly, it is expected

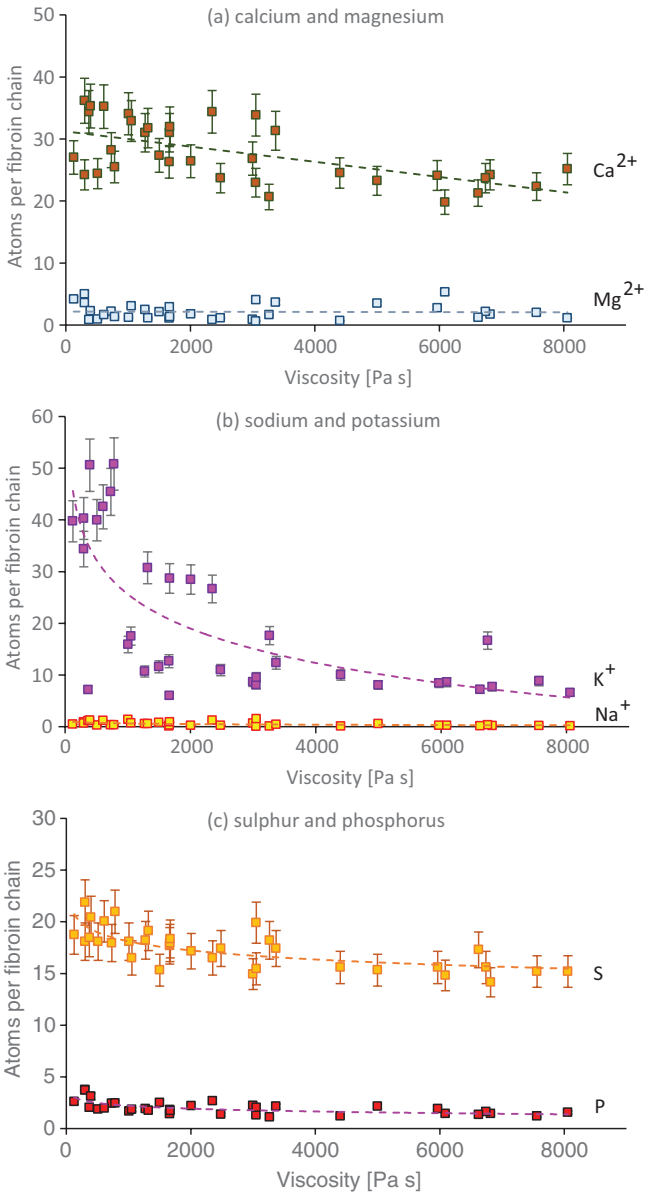

Figure 5. Elemental analyses of cast films versus viscosity of the feedstock, reported as atoms per fibroin chain (with molecular weight 420 kDa, containing roughly 5525 amino acids[32]): a) divalent cations: calcium and magnesium; b) monovalent cations: sodium and potassium c) potential anions: sulfur and phosphorus.

that formation of ionic bridges between fibroin chains would increase the viscosity of the feedstock, in line with theory[57,58] and observations on numerous synthetic polymer systems.[59–68]

While the concentrations of divalent ions remained fairly constant throughout cocoon construction, large changes were observed in the concentrations of monovalent cations, particularly K^+ (Figure 5b), which clearly correlated with the viscosity. This ranged from around nine atoms per chain in the higher viscosity samples to more than 40 atoms per chain in the lower viscosity samples. Although the equilibrium is expected to favor bonding to divalent cations, monovalent cations may compete for anions, including those involved in ionic bridging between fibroin chains. Moreover, elevated ionic content would also increase the charge screening around the carboxylate groups.[69] Hence, it is expected that the increase in K^+ concentration could decrease the strength or abundance of ionic bridges between fibroin chains and explain the progressive decrease in viscosity observed during cocoon construction.

Although Na^+ is also expected to compete for anions, its concentration was much lower than K^+ (equivalent to less than 1.5 atoms per chain). Consequently, while a similar correlation was observed between viscosity and the Na^+ concentration, this was expected to have a negligible effect. Hence, we suggest that the K^+ concentration may be the primary modifier of the silk feedstock viscosity.

Previous publications[50–53] have suggested that silk proteins, including fibroin, may undergo phosphorylation (i.e., addition of a phosphate ester group) as a post-translational modification. Irrespective of feedstock viscosity or silk produced, however, the present work found levels of phosphorus equivalent to less than three atoms per fibroin chain (Figure 5c), which placed an upper limit on any phosphorylation that could have occurred on the MP gland contents. Larger amounts of sulfur were detected (equivalent to around 15 atoms per chain in the higher viscosity specimens, rising to around 20 atoms per chain in the lower viscosity specimens). Of these, however, 14 atoms per chain are expected to be associated with sulfur-containing amino acids (Cys and Met[32]). Hence, the apparently modest change in overall level implied a considerable rise in additional sulfur-containing groups as cocoon construction progressed and the feedstock viscosity decreased. It should be emphasized, however, that the present analyses were unable to discriminate between post-translational modification or low molecular weight species, such as phosphate and sulfate anions. Consequently, the changes in sulfur concentration may indicate counter-ions associated with the potassium. This is a potentially important issue, since the counter-ions may also affect the Ca^{2+} activity, which is an avenue for future study.

3.5. Infrared Spectroscopy

While the interplay between K^+ and Ca^{2+} is proposed to be the main influence for the changes in feedstock rheology during cocoon construction, other potential compositional changes (including anions or other small molecules) were investigated by IR spectroscopy. A typical full range spectrum is shown in **Figure 6**a. Despite using thin films, the strongest bands (O—H and N—H stretching, around 3300 cm^{-1} and the amide bands around 1640 and 1540 cm^{-1}) were still frequently too intense, leading to peak distortion and "clipping." Nevertheless, as all the samples were predominantly protein, these intense bands were of less interest in the present investigation.

Significant changes were observed in the fingerprint region (between 1500 and 800 cm^{-1}), as shown in Figure 6b. In particular, after normalizing on the amide III band (1243 cm^{-1}) to compensate for differences in film thickness, it was found that spectra from higher viscosity specimens (>4000 Pa s, shown in blue) tended to be more intense between 1170 and 992 cm^{-1}, while those corresponding to lower viscosities (<400 Pa s, shown in magenta) were more intense between

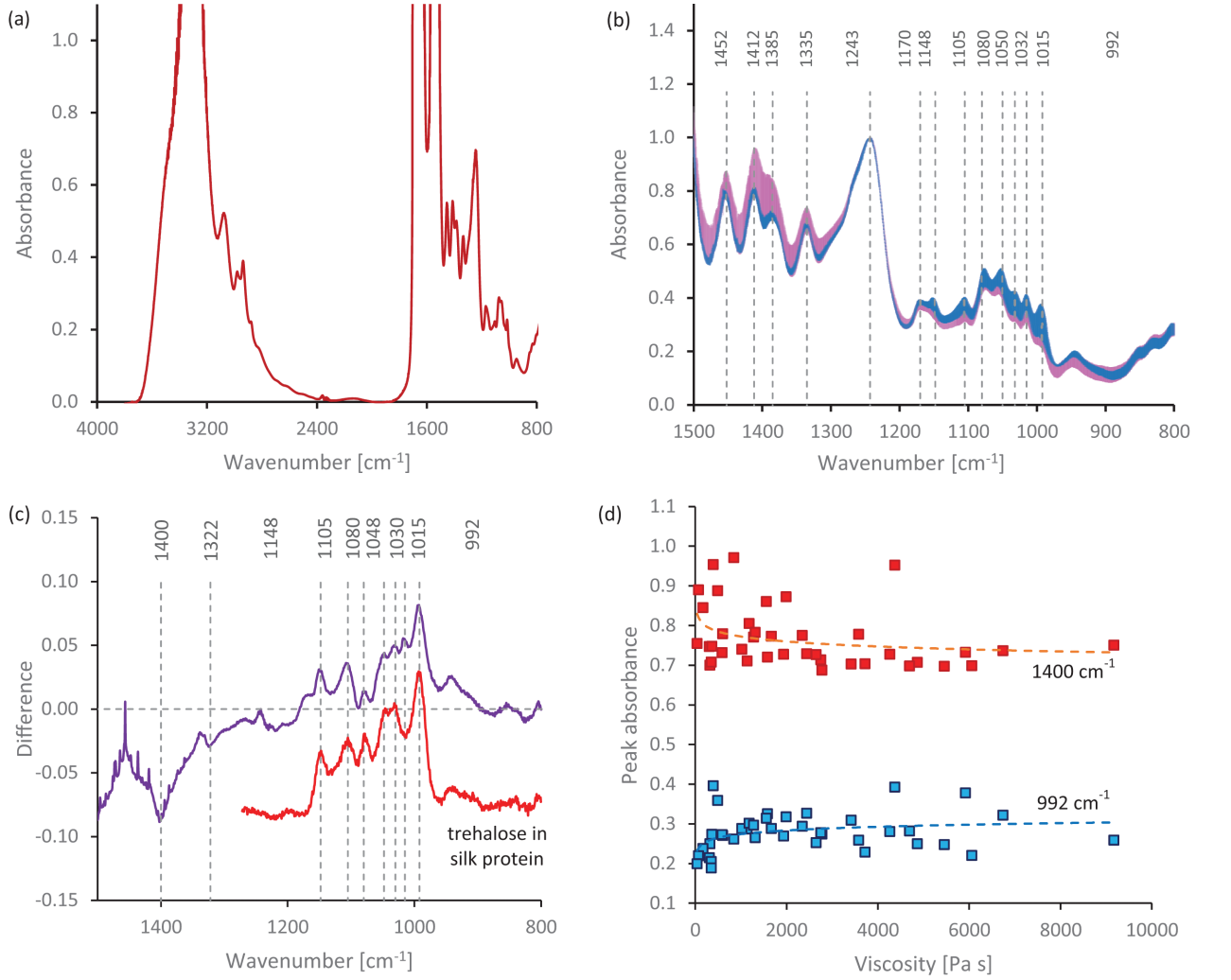

Figure 6. Analysis of silk solid residue by FTIR: a) full range spectrum collected in transmission mode; b) "fingerprint region" spectra from highest (>4000 Pa s, in blue) and lowest viscosity films (<400 Pa s, in magenta), after normalizing with respect to the amide III band (1243 cm^{-1}); c) averaged difference (blue-magenta, highest–lowest viscosity) from the spectra shown in (b), with a portion of a trehalose reference spectrum (red); d) changes in absorbance at 992 cm^{-1} (blue) and 1400 cm^{-1} (red) versus viscosity of the silk feedstock.

1500 and 1243 cm^{-1}. This is also shown as a "difference spectrum" (highest–lowest viscosities) in Figure 6c.

Phosphorylation has been reported previously as a significant post-translational modification of silk fibroin,[51–53] although it appears to have been largely overshadowed by the elemental analyses in the present work. The strongest absorbance band of the phosphate group is expected around 1080 cm^{-1}, with a slightly weaker band between 970 and 990 cm^{-1}.[70,71] While close examination revealed bands in these regions, in the IR spectra from all the samples prepared here, this cannot be regarded as proof that phosphorylation was responsible for the spectroscopic or rheological changes. First, the attribution of these peaks to phosphate groups is uncertain. Although the peak at 1080 cm^{-1} was larger than that at 992 cm^{-1} in Figure 6b (as expected for phosphate), the opposite was observed in the difference spectrum (Figure 6c). This implies that, even if phosphate were present, there must have been other contributions to the peak at 992 cm^{-1}. Indeed, Boulet-Audet et al.[72] previously attributed a band at 998 cm^{-1} to glycine >CH2 rocking modes from $(Ala\text{-}Gly)_n$ segments within β-sheets, which could have affected the apparent height of the peak observed at 992 cm^{-1}. Moreover, phosphate groups would account for only 2 peaks, whereas the difference spectrum revealed at least 8 peaks between 992 and 1243 cm^{-1}.

An alternative interpretation of the increased IR absorbance between 992 and 1243 cm^{-1} could be the presence of carbohydrates. In general, all carbohydrates (as simple sugars or more complex polysaccharides) absorb strongly in this region, due to various group and combination modes, which depend on the sugar type (i.e., the substitution pattern and stereochemistry around the sugar ring).[73–75] These carbohydrates may have been present as cosolutes within the feedstock or in the form of protein glycosylation.[76,77] Indeed, it has been suggested that the P25 silk protein may contain *N*-linked mannose-based oligosaccharide chains, although fibroin does not appear to be glycosylated.[78]

A more plausible explanation, however, appears to be the presence of trehalose (a nonreducing disaccharide with α,α-1,1-linked glucose rings) in the silk protein samples. This is the main hemolymph sugar in many insects[79] and has been observed in the silk glands of *B. mori* with a peak concentration of 12 μmole g^{-1} (equivalent to 1.6 wt% on dry weight of protein) just prior to the start of fiber spinning.[80–83] Consistent with this, a reference spectrum of trehalose (prepared by augmenting silk protein films with the sugar) gave a good match for 7 of the 9 peaks between 900 and 1200 cm^{-1}, as demonstrated in Figure 6c.

By comparison, poorer matches were obtained with the spectra expected for glucose or other sugars that might be present.[74] While this gave strong support for the presence of trehalose, however, it is not conclusive, due to similarities between the IR spectra of some sugars and the possible presence of other compounds with absorbance bands in the same region.

Plotting the height of the strongest peak in this region (at 992 cm^{-1}) indicated considerable variability between specimens, as shown in Figure 6d. Nevertheless, a slight trend of lower absorbance toward lower viscosities appeared to be consistent with previous reports of decreasing trehalose concentration during cocoon construction.[82,83] In view of the weak correlation and the relatively low concentration of trehalose expected (up to around 0.4 wt% in the feedstock), however, this seems unlikely to explain the changes in viscosity observed. As trehalose is the main metabolic sugar in silkworms and other insects,[79–83] its presence in the feedstock may be a result of increased cellular respiration during fibroin synthesis. Trehalose may also contribute toward protein stabilization and hydration.[79,84]

On the other hand, lower viscosity specimens appeared to be associated with a broad peak around 1400 cm^{-1} and a smaller peak around 1322 cm^{-1} (negative peaks in Figure 6c). Absorbance bands between 1280 and 1500 cm^{-1} have been ascribed to the various C—H bending modes abundant in protein specimens;[72,85,86] however, it is uncertain why these should be more intense in films from the lower viscosity specimens. Alternatively, strong absorbance bands around 1325 and 1400 cm^{-1} have been reported for ammonium bicarbonate,[87] which may provide a more plausible explanation for these spectral changes. The absorbance at 1400 cm^{-1} (Figure 6d) increased toward lower viscosity, suggesting some similarity to the change in K^+ concentration (Figure 5b). Hence, this may be due to the counter-ion, which may be an area for future work.

3.6. Changes in Fibroin Molecular Weight

Previously, variations in the length (or molecular weight) of the fibroin molecule[88] and changes in the proportions of different proteins in native silk feedstocks have been observed.[89,90] Hence, SDS-PAGE was used to investigate whether the changes in rheology of the silk feedstock during the cocoon construction process may have been linked to differences in protein length or composition (**Figure 7**). Analyses under reducing conditions revealed two main protein bands around 440 ± 60 and 24 ± 3 kDa in the feedstock specimens, which were ascribed to the heavy and light sections of fibroin (Fib-H and Fib-L) respectively.[91,92] These results for Fib-H were somewhat higher than the expected value (391.4 kDa), based on the amino acid sequence.[32] This may be due to differences in migration of such high molecular weight fibrillar proteins in relation to their globular markers; thus, an uncertainty of around ± 60 kDa was estimated. At the same time, the present results for Fib-L agreed fairly well with the expected value (25–27.7 kDa) based on other electrophoresis measurements and genetic sequencing studies.[30–32,91,92]

On balance, irrespective of their absolute values, both Fib-H and Fib-L exhibited constant molecular masses throughout the stages of cocoon construction (Figure 7c) and irrespective of shear viscosity (Figure 7d). Thus, the observed variation in viscosity could not be attributed to changes in the chain lengths of these proteins.

In some cases, additional faint bands were observed (e.g., see tracks 6 and 7 in Figure 7a), which may have been due to the presence of sericin. Nevertheless, the faintness of these bands suggested relatively small amounts, compared with the fibroin, and no correlation was observable with the feedstock viscosity.

4. Discussion

This work has provided a much clearer picture of the considerable variability in viscosity reported previously[18,19] for silk feedstocks. It is now apparent that these changes occur prior to and during cocoon construction, as a result of systematic changes in feedstock composition, rather than merely as random variations in a poorly controlled material. This is more consistent with the usual expectations of exquisite control in biological systems, rather than the chaotic picture suggested by apparently disparate viscosity data in previous reports.[18,19] Clearly, at least some of that apparent chaos could arise due to the condition of the silkworm and its progress through cocoon construction.

Several compositional changes were identified, which may be related to metabolic changes prior to or during cocoon construction (such as hemolymph pH and trehalose concentration), but were unlikely to be the main cause of changes to the feedstock rheology. Instead, it is more likely that both of these changes were related to the silkworm's requirements to maximize fibroin production prior to cocoon construction—using ammonia as a nitrogen source[26,27] and trehalose as fuel for the cellular mechanisms.[79–83]

On the other hand, it is likely that the elemental compositions of the feedstock, particularly the relative concentrations of divalent and monovalent cations (mainly Ca^{2+} and K^+) did affect the rheology, through salt bridges between fibroin chains. In this respect, it is informative to consider the possible balance between cations and anions. Fibroin is expected to contribute around 77 carboxylic acid groups per chain,[32] in the form of acidic amino acids (Asp and Glu)—roughly sufficient to balance all the cations observed in the higher viscosity specimens. As Ca^{2+} (and Mg^{2+}) carboxylate salts are only weakly dissociated,[54,55,93] they may be expected to form relatively stable bridges between different protein chains. Although this appeared to be insufficient to fully gel the silk feedstock (i.e., these samples still flowed), it could explain the higher viscosities observed.

Perhaps the most obvious example of complexation between carboxylate groups and divalent cations arises in the spinning of

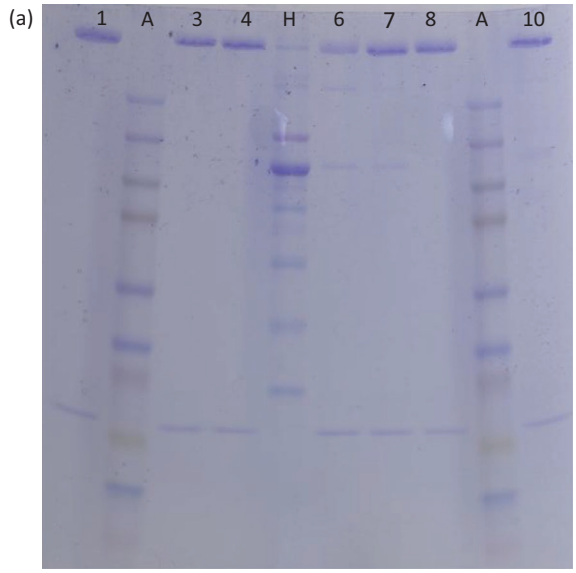

(b)

Lane	Sample identity; feedstock viscosity [Pa s]	Main bands seen [kDa]
A	Amersham rainbow standards	12, 17, 24, 31, 38, 52, 76, 102, 150, 225
H	Hi-Mark standards	31, 41, 55, 71, 117, 171, 238, 268, 460
1	566	24, 442
3	3392	24, 445
4	1811	24, 458
6	955	24, 123, 438
7	703	24, 124, 431
8	116	25, 446
10	464	24, 450

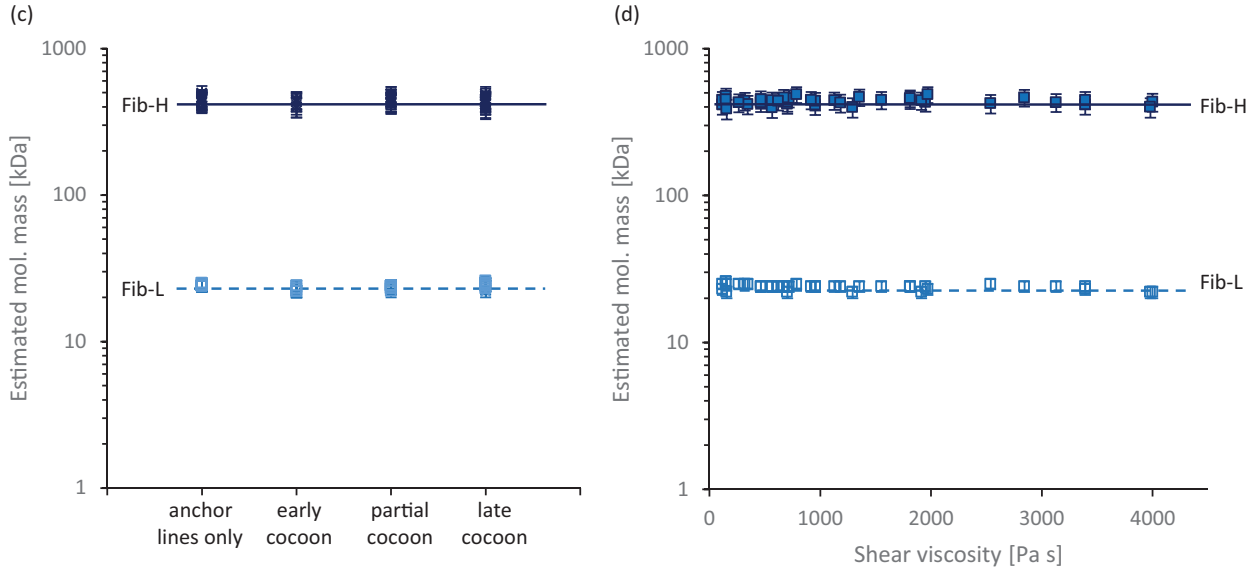

Figure 7. Analysis of silk feedstock proteins by PAGE: a) example of a gel (as shown here, the specimens were loaded at the top of the image and the bands moved downward); b) table showing identities of specimens in each lane and the main bands observed; c,d) estimated molecular weights of Fib-H and Fib-L proteins related to cocoon construction stage or feedstock viscosity.

alginate fibers,[94] where replacing Na^+ ions by Ca^{2+}, causes coagulation of the insoluble polysaccharide (a copolymer of mannuronic and guluronic acids from brown seaweed). The possibility of salt bridges between carboxylate side-groups of fibroin chains has been suggested previously by Iizuka.[14] More recently, evidence for specific interactions between cations and side-groups of acidic amino acids in proteins has been published elsewhere. For example: Brown et al.[95] reported Asp in the Ca-binding domains of integrin, while Gao et al.[96] reported the involvement of Asp and Glu in the binding of Ca by Hahellin.

In essence, the higher viscosity might represent silk feedstock under "storage conditions," before it is required for spinning. Subsequently, the rise in the concentration of monovalent cations (i.e., K^+) would displace some of the divalent ions from the carboxylate salts and increase electrostatic screening around anionic groups,[69] reducing the amount of interchain bridging and lowering the viscosity. If correct, this mechanism represents a chemically simple method by which the silkworm can alter the viscosity of the feedstock, by controlling the ion concentration in the gland via its own ion-transport proteins,[49] using species abundant in its foodstuff (mulberry leaves).[97,98]

While theoretical treatments of the rheological effects due to temporary physical crosslinks between polymer chains have been presented elsewhere;[58,59] a more specific treatment of salt bridges between fibroin chains will be given in the forthcoming paper by Schaefer et al.[20]

Finally, it should be emphasized that the work presented here only considered changes in the MP section of the gland,

which appears to provide feedstock storage until required and before significant sericin content is added. These results may not apply directly to the feedstock that actually emerges from the spinneret. Indeed, several authors have reported systematic changes in ion content during passage toward the spinneret[47–49] and corresponding changes in viscosity may be anticipated. Calculations based on the most recent data by Wang et al.[49] suggest that calcium decreases from around 30 to about 5 atoms per chain, while potassium increases from around 30 to 115 atoms per chain, as the feedstock moves from the MP to the anterior section. According to the hypothesis presented here, this should produce a significant reduction in viscosity, although more quantitative predictions are not currently possible. Investigating the composition and flow behavior closer to the spinneret currently represents a significant technical challenge; nevertheless, this merits closer examination and will be the subject of further work.

5. Conclusions

This work investigated the compositional changes in silk feedstock from *B. mori*, revealing a potential explanation for the rheological changes observed previously. Rather than random changes in a poorly controlled material, it was found that the viscosity of feedstock specimens from the MP gland division decreased systematically, prior to and during cocoon construction. This appeared to be controlled through competition between divalent (mainly Ca^{2+}) and monovalent (mainly K^{+}) ions, which is expected to affect the strength of salt bridging between acidic amino acids (Asp and Glu) of the fibroin chains. This chemically simple yet sophisticated method is more in keeping with the exquisite control usually expected in biological systems, rather than the variability suggested by data in previous reports.

Acknowledgements

This work was funded by the EPSRC (SPICE, project reference EP/K005693/1) and EU (Horizon 2020, FLIPT 713475) grants. In line with the publishing requirements of those funders, the experimental data used in constructing the figures in this paper are available from the Online Research Data website of the University of Sheffield: https://orda.shef.ac.uk/. The authors are also grateful to Neil Bramall (Department of Chemistry. University of Sheffield) for performing the OES analyses and to Dr. Charley Schaefer and Prof. Tom McLeish (University of York) for helpful comments during the preparation of this manuscript.

Conflict of Interest

The authors declare no conflict of interest.

Keywords

cocoon construction, composition, rheology, silk feedstock

Received: May 21, 2018
Revised: June 25, 2018
Published online: July 24, 2018

[1] C. L. Craig, *Annu. Rev. Entomol.* **1997**, *42*, 231.
[2] A. A. Walker, C. Holland, T. D. Sutherland, *Proc. Roy. Soc. B.* **2015**, *282*, 20150259.
[3] M. Andersson, J. Johansson, A. Rising, *Int. J. Mol. Sci.* **2016**, *17*, 1290.
[4] T. D. Sutherland, J. H. Young, S. Weisman, C. Y. Hayashi, D. J. Merritt, *Annu. Rev. Entomol.* **2010**, *55*, 171.
[5] F. Sehnal, T. Sutherland, *Prion* **2008**, *2*, 145.
[6] E. Doblhofer, A. Heidebrecht, T. Scheibel, *Appl. Microbiol. Biotechnol.* **2015**, *99*, 9361.
[7] D. Ebrahimi, O. Tokareva, N. G. Rim, J. Y. Wong, D. L. Kaplan, M. J. Buehler, *Biomat. Sci. Eng.* **2015**, *1*, 864.
[8] F. Vollrath, D. Porter, C. Holland, *MRS Bull.* **2013**, *38*, 73.
[9] C. Fu, Z. Shao, F. Vollrath, *Chem. Comm.* **2009**, *43*, 6515.
[10] F. Vollrath, D. Porter, *Soft Matter* **2006**, *2*, 377.
[11] J. Pérez-Rigueiro, C. Viney, J. Llorca, M. Elices, *J. App. Poly. Sci.* **2000**, *75*, 1270.
[12] C. Holland, F. Vollrath, A. J. Ryan, O. Mykhaylyk, *Adv. Mats.* **2012**, *24*, 105.
[13] J. Sparkes, C. Holland, *Nature Comms.* **2017**, *8*, 594.
[14] E. Iizuka, *J. Appl. Polym. Sci. Appl. Polym. Symp.* **1985**, *41*, 173.
[15] E. Iizuka, *Biorheology* **1996**, *3*, 141.
[16] C. Foà, *Kolloid Z.* **1912**, *10*, 7.
[17] P. R. Laity, C. Holland, *Int. J. Mol. Sci.* **2016**, *17*, 1812.
[18] P. R. Laity, C. Holland, *Biomacromolecules* **2016**, *17*, 2662.
[19] P. R. Laity, S. E. Gilks, C. Holland, *Polymer* **2015**, *67*, 28.
[20] C. Schaefer, P. R. Laity, C. Holland, T. C. B. McLeish, unpublished.
[21] N. J. Harrick, *J. Phys. Chem.* **1960**, *64*, 1110.
[22] S. Ekgasit, A. Padermshoke, *Appl. Spectr.* **2001**, *55*, 1352.
[23] M. Boulet-Audet, T. Buffeteau, S. Boudreault, N. Daugey, M. Pézolet, *J. Phys. Chem. B.* **2010**, *114*, 8255.
[24] T. Buffeteau, B. Desbat, D. Eyquem, *Vib. Spectr.* **1996**, *11*, 29.
[25] H. Wang, N. Mao, X. Hu, H. Shao, X. Jin, *J. Wuhan Univ. Technol. Mater. Sci. Ed.* **2011**, *26*, 262.
[26] C. Hirayama, M. Sugimura, H. Saito, M. Nakamura, *J. Insect Physiol.* **2000**, *46*, 1415.
[27] C. Hirayama, K. Konno, H. Shinbo, *J. Insect Physiol.* **1996**, *42*, 983.
[28] C.-Z. Zhou, F. Confalonieri, N. Medina, Y. Zivanovic, C. Esnault, T. Yang, M. Jacquet, J. Janin, M. Duguet, R. Perasso, Z.-G. Li, *Nucl. Acids Res.* **2000**, *28*, 2413.
[29] C.-Z. Zhou, F. Confalonieri, M. Jacquet, R. Perasso, Z.-G. Li, J. Janin, *Proteins: Struct. Func. Gen.* **2001**, *44*, 119.
[30] K. Tanaka, N. Kajiyama, K. Ishikura, S. Waga, A. Kikuchi, K. Ohtomo, T. Takagi, S. Mizuno, *Biochim. Biophys. Acta* **1999**, *1432*, 93.
[31] K. Yamaguchi, Y. Kikuchi, T. Takagi, A. Kikuchi, F. Oyama, K. Shimura, S. Mizuno, *J. Mol. Biol.* **1989**, *210*, 127.
[32] GenBank overview, https://www.ncbi.nlm.nih.gov/genbank/ (accessed: May **2018)**.
[33] L. J. Domigan, M. Andersson, K. A. Alberti, M. Chesler, Q. Xu, J. Johansson, A. Rising, D. L. Kaplan, *Insect Biochem. Mol. Biochem.* **2015**, *65*, 100.
[34] S. Bai, S. Liu, C. Zhang, W. Xu, Q. Lu, H. Han, D. L. Kaplan, H. Zhu, *Acta Biomat.* **2013**, *9*, 7806.
[35] X.-Y. He, N.-N. Zhang, W.-F. Li, N. Jia, B.-Y. N. Chen, K. Zhou, J. Zhang, Y. Chen, C.-Z. Zhou, *J. Mol. Biol.* **2012**, *418*, 197.
[36] P. Zhou, X. Xie, D. P. Knight, X.-H. Zong, F. Deng, W.-H. Yao, *Biochemistry* **2004**, *43*, 11302.
[37] C. Dicko. J. M. Kenny, D. Knight, F. Vollrath, *Biochemistry* **2004**, *43*, 14080.
[38] T. K. Harris, G. J. Turner, *Life* **2002**, *53*, 85.
[39] T. Asakura, Y. Watanabe, A. Uchida, H. Minagawa, *Macromolecules* **1984**, *17*, 1075.
[40] T. Asakura, H. Suzuki, Y. Watanabe, *Macromolecules* **1983**, *16*, 1024.
[41] A. E. Terry, D. P. Knight, D. Porter, F. Vollrath, *Biomacromolecules* **2004**, *5*, 768.

[42] M. Doi, S. F. Edwards, *Theory of Polymer Dynamics*, Clarendon Press, Oxford, **1986**.
[43] G. C. Berry, T. G. Fox, *Adv. Polym. Sci.* **1968**, *5*, 261.
[44] M. Adam, M. Delsanti, *J. Physique* **1983**, *44*, 1185.
[45] V. R. Raju, E. V. Menezez, G. Marin, W. W. Graessley, L. J. Fetters, *Macromolecules* **1981**, *14*, 1668.
[46] S. Onogi, T. Masuda, N. Miyanaga, Y. Kimura, *J. Polym. Sci. A2* **1967**, *5*, 899.
[47] L. Zhou, A. E. Terry, Y. Huang, Z. Shao, X. Chen, *Acta Chim. Sinica* **2005**, *63*, 1379.
[48] L. Zhou, X. Chen, Z. Shao, Y. Huang, D. P. Knight, *J. Phys. Chem. B.* **2005**, *109*, 16937.
[49] X. Wang, Y. Li, Q. Liu, Q. Chen, Q. Xia, P. Zhao, *Biochim. Biophys. Acta* **2017**, *1861*, 567.
[50] M. Mann, O. N. Jensen, *Nature Biotech.* **2003**, *21*, 255.
[51] J.-Y. Li, H.-J. Yang, T.-Y. Lan, H. Wei, H.-R. Zhang, M. Chen, W. Fan, Y.-Y. Ma, B.-X. Zhong, *J. Proteome Res.* **2011**, *10*, 3551.
[52] W.-Q. Chen, H. Priewalder, J. P. P. John, G. Lubec, *Proteomics* **2010**, *10*, 369.
[53] P. Zhang, Y. Aso, K. Yamamoto, Y. Banno, Y. Wang, K. Tsuchida, Y. Kawaguchi, H. Fujii, *Proteomics* **2006**, *6*, 2586.
[54] G. J. Millar, S. Papworth, S. J. Couperthwaite, *Desalination* **2014**, *351*, 27.
[55] R. Kohn, I. Furda, A. Haug, O. Smidsrød, *Acta Chem. Scand.* **1968**, *22*, 3098.
[56] N. N. Ashton, D. R. Roe, R. B. Weiss, T. E. Cheatham, R. J. Stewart, *Biomacromolecules* **2013**, *14*, 3668.
[57] Q. Chen, Z. Zhang, R. H. Colby, *J. Rheol.* **2016**, *60*, 1031.
[58] L. Leibler, M. Rubinstein, R. H. Colby, *Macromolecules* **1991**, *24*, 4701.
[59] R. Stadler, L. de Lucca Freitas, *Macromolecules* **1989**, *22*, 714.
[60] R. Stadler, L. de Lucca Freitas, *Coll. Poly. Sci.* **1988**, *266*, 1102.
[61] R. Stadler, L. de Lucca Freitas, *Coll. Polym. Sci.* **1986**, *264*, 773.
[62] L. de Lucca Freitas, R. Stadler, *Macromolecules* **1987**, *20*, 2478.
[63] L. de Lucca Freitas, R. Stadler, *Coll. Polym. Sci.* **1988**, *266*, 1095.
[64] L. de Lucca Freitas, J. Burgert, R. Stadler, *Polym. Bull.* **1987**, *17*, 431.
[65] A. E. González, *Polymer* **1984**, *25*, 1469.
[66] A. E. González, *Polymer* **1983**, *24*, 77.
[67] N. Z. Erdi, H. Morawetz, *J. Coll. Sci.* **1964**, *19*, 708.
[68] R. Longworth, H. Morawetz, *J. Polymer Sci.* **1958**, *29*, 307.
[69] E. Jordan, F. Roosen-Runge, S. Leibfarth, F. Zhang, M. Sztucki, A. Hildebrandt, O. Kohlbacher, F. Schreiber, *J. Phys. Chem. B.* **2014**, *118*, 11365.
[70] L. Chen, H.-Y. N. Holman, Z. Hao, H. A. Bechtel, M. C. Martin, C. Wu, S. Chu, *Anal. Chem.* **2012**, *84*, 4118.
[71] P. Garidel, H. Schott, *BioProcess International* **2006**, *4*, 48.
[72] M. Boulet-Audet, F. Vollrath, C. Holland, *J Exp. Biol.* **2015**, *218*, 3138.
[73] E. Wiercigroch, E. Szafraniec, K. Czamara, Z. Mrta, M. Z. Pacia, K. Majzner, K. Kochan, A. Kaczor, M. Baranska, K. Malek, *Spectrochim. Acta* **2017**, *185*, 317.
[74] M. Kanou, K. Nakanishi, A. Hashimoto, T. Kameoka, *Appl. Spectr.* **2005**, *59*, 885.
[75] M. Kaćuráková, R. H. Wilson, *Carbohydr. Polym.* **2001**, *44*, 291.
[76] M. Khajehpour, J. L. Dashnau, J. M. Vanderkooi, *Anal. Biochem.* **2006**, *348*, 40.
[77] A. Natalello, D. Ami, S. Brocca, M. Lotti, S. M. Doglia, *Biochem. J.* **2005**, *385*, 511.
[78] K. Tanaka, S. Inoue, S. Mizuno, *Insect Biochem. Mol. Biol.* **1999**, *29*, 269.
[79] S. N. Thompson, *Adv. Insect Phys.* **2003**, *31*, 205.
[80] G. R. Wyatt, T. C. Loughheed, S. S. Wyatt, *J. Gen. Physiol.* **1956**, *39*, 853.
[81] G. R. Wyatt, G. F. Kalf, *J. Gen. Physiol.* **1957**, *40*, 833.
[82] S. Shimada, M. Kido, A. Kamada, S. Asano, *Insect Biochem.* **1980**, *10*, 175.
[83] T. Furusawa, T. Wakizaka, Y. Ishihara, *Appl. Entomol. Zool.* **1993**, *28*, 169.
[84] N. K. Jain, I. Roy, *Protein Sci.* **2009**, *18*, 24.
[85] A. Barth, *Prog. Biophys. Mol. Biol.* **2000**, *74*, 141.
[86] A. Barth, *Biochim. Biophys. Acta* **2007**, *1767*, 1073.
[87] F. A. Miller, C. H. Wilkins, *Anal. Chem.* **1952**, *24*, 1253.
[88] R. F. Manning, L. P. Gage, *J. Biol. Chem.* **1980**, *255*, 9451.
[89] Z. Dong, P. Zhao, C. Wang, Y. Zhang, J. Chen, X. Wang, Y. Lin, Q. Xia, *J. Proteome Res.* **2013**, *12*, 5213.
[90] Z. Dong, P. Zhao, Y. Zhang, Q. Song, X. Zhang, P. Guo, D. Wang, Q. Xia, *Sci. Reps.* **2016**, *6*, 21158.
[91] K. Tanaka, K. Mori, S. Mizuno, *J. Biochem.* **1983**, *114*, 1.
[92] H. Yamada, H. Nakao, Y. Takasu, K. Tsubouchi, *Mat. Sci. Eng. C.* **2001**, *14*, 41.
[93] I. Greenwald, *J. Biol. Chem.* **1938**, *124*, 437.
[94] Y. Qin, *Polym. Int.* **2008**, *57*, 171.
[95] K. L. Brown, S. Banerjee, A. Feigley, H. Abe, T. S. Blackwell, A. Pozzi, B. G. Hudson, R. Zent, *Sci. Reps.* **2018**, *8*, 2916
[96] M. Gao, F. Yang, L. Zhang, Z. Su, Y. Huang, *J. Biomol. Struct. Dynam.* **2018**, *36*, 1171.
[97] F. Chen, J. Lu, M. Zhang, K. Wan, D. Liu, *J. Plant Nutr. Soil Sci.* **2009**, *172*, 245.
[98] D. Yigit, F. Akart, E. Baydas, M. Buyukyildiz, *Asian J. Chem.* **2010**, *22*, 3554.